ChemPubSoc Europe

DOI: 10.1002/slct.201801781

Chemistry SELECT Full Papers

Materials Science inc. Nanomaterials & Polymers

SERS of Trititanate Nanotubes: Selective Enhancement of Catechol Compounds

Ruochen Liu,[a, b] Edmund Morris,[a, b] Xiaorong Cheng,[c] Eric Amigues,[a] Kim Lau,[a] Baekman Kim,[a] Yuanhang Liu,[a] Zhipeng Ke,[d] Sharon E. Ashbrook,[d] Michael Bühl,[d] and Graham Dawson*[a]

The surface enhanced Raman scattering of trititanate nanotubes (TiNT) modified with enediol ligands was investigated and it was found that the functional group dramatically affects the enhancement observed. For TiNT-4-nitrocatechol, a SERS enhancement is seen; however, when dopamine is attached, no signal is seen. The relative band gap positions upon 785 nm laser excitation are proposed to explain the observed phenomenon. This attachment is investigated by solid state NMR and UV/Vis spectroscopy and supported by DFT calculations to offers further insights into catechol coatings of nanomaterials and SERS by the chemical method. We expect this non noble metal containing composite material to have applications in bioimaging and bio and chemical detection.

Introduction

Semiconducting inorganic nanostructures[1,2] have been extensively investigated for applications in photocatalysis, energy storage and biomedical probes. Within this field, TiO_2 has received considerable interest due to its photocatalytic properties,[3,4] which include high oxidative power and long term stability. In 1998, Kasuga *et al.* reported the preparation of titania nanotubes[5] through the hydrothermal treatment of TiO_2 with 10 M NaOH. These nanotubes had a porous structure and high surface area. The composition of the nanotubes was subsequently identified as trititanate,[6–9] $H_2Ti_3O_7$. We have modified these nanotubes with dopamine, which imbued the nanotubes with photocatalytic properties. This caused the promotion of electron injection and charge separation and added activity to the unmodified system.[10] The modification resulted in a colour change and a shoulder in the UV-vis spectrum, stemming from the created charge transfer complex. With a view to biomedical applications, this was further investigated using ssNMR and XRD to discern if any degree of polymerisation had occurred. Our study found that the dopamine molecules attached as monomer units through either a monodentate or bidentate mode of binding.[11]

Surface enhanced Raman scattering (SERS) is a powerful analytical technique for chemical sensing of trace amounts of analyte, providing in-depth structural information. Most SERS results published to this date have used metallic, particularly silver and gold, nanoparticles and the enhancement has come from a mixture of the surface plasmon resonance of the metal nanoparticles and a charge transfer resonance involving the transfer of electrons between the molecule and the conduction band of the metal. A third contribution comes from the resonances within the molecule itself- the chemical method,[12] however the exact mechanism is still a source of debate. Semiconductor SERS has been reported[13,14] for TiO_2 as well as other semiconductors.[15,16] The chemical method requires a specific interaction between the adsorbed molecules and the surface, and forms a charge transfer complex which absorbs light at the excitation wavelength, producing resonance Raman scattering.[13] The plasmon resonance frequency of most semiconductors is either in the infrared region or of poor quality due to coupling between the conduction electrons and the interband electronic transitions,[17] however this type of SERS has been shown for TiO_2 nanoparticles modified with enediol catechol ligands.[13,14] In this system nontotally symmetric vibrations lead to deviations in the symmetry of the modifier and are necessary for the charge transfer transitions and, therefore, the surface enhancement.

The chemical method of SERS is often described by the photo-induced charge transfer (PICT) process, however when a surface complex is involved the Surface Complexes Resonance Enhancement mechanism is the most appropriate explanation. Complexes formed by the chemisorption of molecules on the substrate surface form new highest occupied molecular orbital (HOMO) and lowest unoccupied molecular orbitals (LUMO),

[a] R. Liu, E. Morris, Dr. E. Amigues, Prof. K. Lau, B. Kim, Y. Liu, Dr. G. Dawson
Department of Chemistry, Xian Jiaotong Liverpool University, Suzhou, PR China
E-mail: graham.dawson@xjtlu.edu.cn
[b] R. Liu, E. Morris
Department of Chemistry, University of Liverpool, Crown Street Liverpool
[c] Dr. X. Cheng
Suzhou Institute of Industrial Technology, Suzhou, PR China
[d] Z. Ke, Prof. S. E. Ashbrook, Prof. M. Bühl
School of Chemistry, University of St Andrews

Supporting information for this article is available on the WWW under https://doi.org/10.1002/slct.201801781

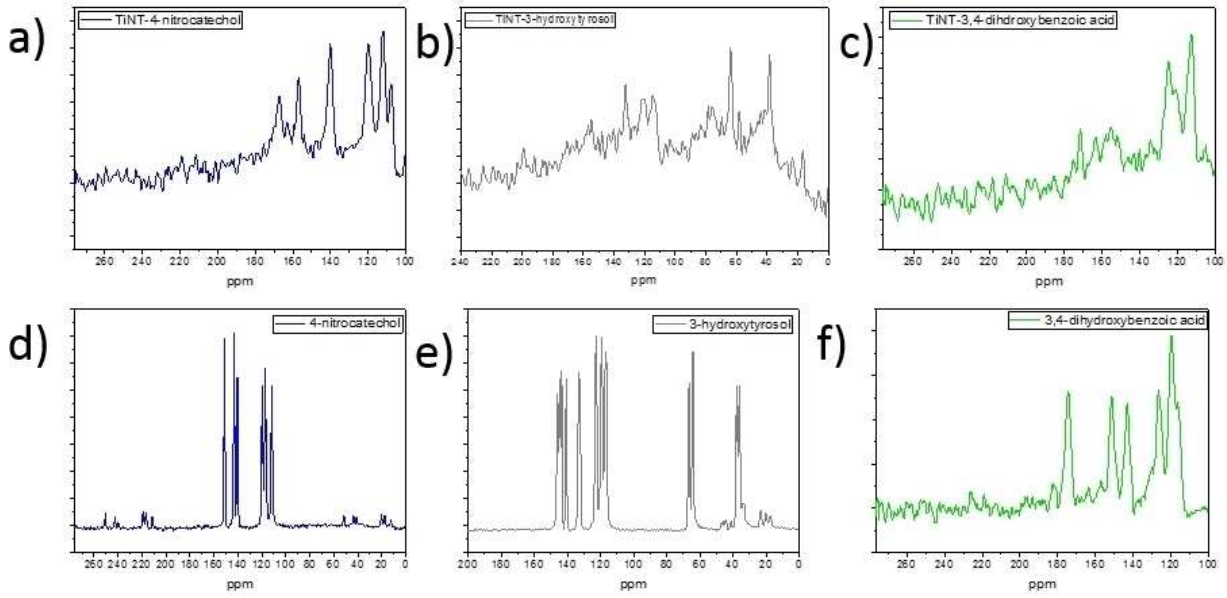

Figure 2. ssNMR spectra of the TiNT-modified samples (a-c) and the starting materials (d-f).

which under suitable excitation show resonance Raman scattering enhancement.[18,19]

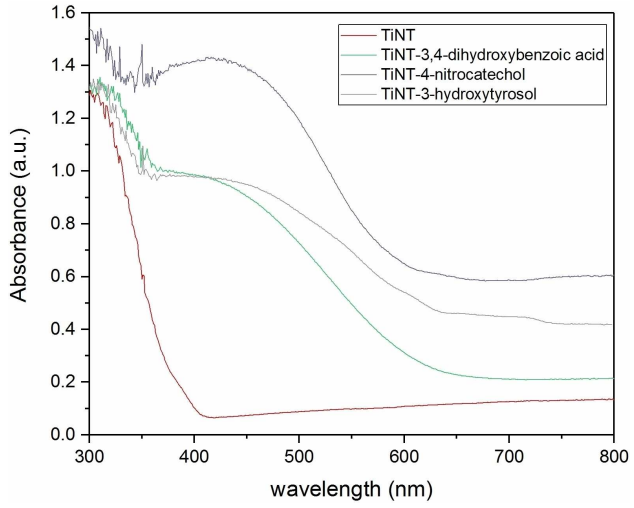

Figure 1. UV/Vis spectra for TiNT and TiNT-modified samples.

The investigation into the SERS properties of various enediol ligands attached to trititanate nanotubes has shown interesting results. These nanotubes have a scroll structure with a diameter of 8 nm and lengths of in excess of 100 nm. We see a dependence on the SERS effect related to the proximity of the functional group to the benzene ring for this system. This study offers further insights into catechol coatings of nanomaterials and SERS by the chemical method. We expect this composite material to have applications in bioimaging[20,21] and in bio and chemical[22,23] detection where the biocompatible nature of the system will be an advantage.[24,25]

Results and Discussion

In our previous work we have proposed mixed bidentate and monodentate *in-situ* structural models for dopamine on trititanate nanotubes using solid state NMR and powder XRD. The dopamine monomer units exist in a close packed arrangement on the nanotube surface.[11] We have previously shown this system to be photocatalytically active.[10] In this current work we have examined the surface enhanced Raman activity of a series of enediol functionalized TiNT systems. The position of the sidechain/functional group is of paramount importance to the SERS effect. Figure 1 shows the solid drs UV/vis of TiNT functionalized by various enediol ligands. As can be observed, all samples show a similar profile: a charge transfer[13] band dominating the visible range of the spectrum with an onset from 600 nm and showing a shoulder leading into the band edge at around 380 nm. The intensity of the shoulder is greatest for the 4-nitroctechol modified sample, however all samples show a similar profile indicating a similar attachment mode for all compounds, which is expected from this selection of organic modifiers. The colour of the samples can be seen in Figure S1. Our calculations have confirmed the existence of charge transfer complexes and will be discussed later.

Solid state NMR:

^{13}C NMR spectra of the modified samples showed attachment through a bidentate or monodentate Ti–O-aromatic C, as previously observed for TiNT-dopamine.[11] This is shown in Figure 2 for TiNT- 4-nitrocatechol (a), TiNT-3-hydroxytyrosol (b) and TiNT-3,4-dihydroxybenzoic acid (c). In all cases a peak shift

to higher ppm values was observed upon functionalization caused by the replacement of C-OH bonds by C-OH–Ti bonds. These findings are corroborated by computation of the ^{13}C NMR chemical shifts of the parent catechol (free and attached to a $Ti_{10}O_{20}$ model cluster, see Supporting Information). These results show that the best fit with the experimental data comes for the configuration that retains one OH group upon binding to the nanotube surface, and is not fully deprotonated. Furthermore, we observed downshifting of an aromatic C signal, ascribed to π-π stacking of the dopamine monomers on the nanotube surface. This is also seen for 3,4-dihydroxybenzoic acid, 3-hydroxytyrosol and 4-nitrocatechol. π-π stacking is supported by the XRD patterns shown in Figure S2.

For the starting material 4-nitrocatechol, shown in Figure 2 (d), the ^{13}C NMR signals are assigned as follows: the two carbon atoms attached to the hydroxyl groups at δ = 143.2 and 151.1 ppm, the nitro functionalized carbon at δ = 140.4 ppm and the other three aromatic carbon atoms at δ = 111.6, 117.2 and 119.6 ppm. Upon functionalization the two hydroxyl carbon signals show a shift to larger ppm values, indicating conversion of the C-OH to C–O-Ti bonds, 156.8 and 167.2 ppm. From our computation of the ^{13}C NMR chemical shifts we can conclude that the 4-nitrocatechol is not fully deprotonated upon binding to titanate surfaces, but most likely retains one of the OH groups (see Figure S12 and S13). The aromatic carbon signals appear at δ = 107.6, 111.8 and 120.1 ppm in the product, all downshifted compared to the starting material. The peak at δ = 140.4 ppm is assigned as the C attached to the nitro group on the aromatic ring.

For the starting material 3-hydroxytyrosol, shown in Figure 2 (e), the ^{13}C NMR are assigned as follows: the carbon atoms in the chain δ = 37.8 and 64.2 ppm, the two carbon atoms attached to the hydroxyl groups at δ = 143.5 and 144.9 ppm, the chain functionalized carbon at δ = 133 ppm and the other three aromatic carbon atoms at δ = 116.8, 119.2 and 122.7 ppm. Upon functionalization the two hydroxyl carbon signals show a shift to larger ppm values, indicating conversion of the C-OH to C–O-Ti bonds, 154.8 and 156.8 ppm. The aromatic carbon signals appear at δ = 114.8, 120.8 and 132.6 ppm in the product. The carbon with the lowest ppm signal downshifted from δ = 116.8 to 114.8 ppm. The carbons on the chain are still present, as is also true for dopamine modification, showing that no cyclisation has occurred.

For the starting material 3,4-dihydroxybenzoic acid, shown in Figure 2 (f), the ^{13}C NMR signals are assigned as follows: the carbon atom in the carboxylic acid group δ = 174.7 ppm, the two carbon atoms attached to the hydroxyl groups at δ = 151.5 and 143.1 ppm, and the four other aromatic carbon atoms at δ = 126 (overlapping 2 peaks), 119.6 and 116.5 ppm. Upon functionalization the carboxylic acid group signal is downshifted to 171.6 ppm. The two hydroxyl carbon signals show a shift to larger ppm values, indicating conversion of the C-OH to C–O-Ti bonds, 156 and 163.6 ppm. The aromatic carbon signals are all downshifted to δ = 124.8, 121, 112 and 105 ppm.

For the three structures shown in Figure 3, structures a-c, ssNMR and XRD show attachment through the proposed mechanism depicted generally in Figure 3 d.

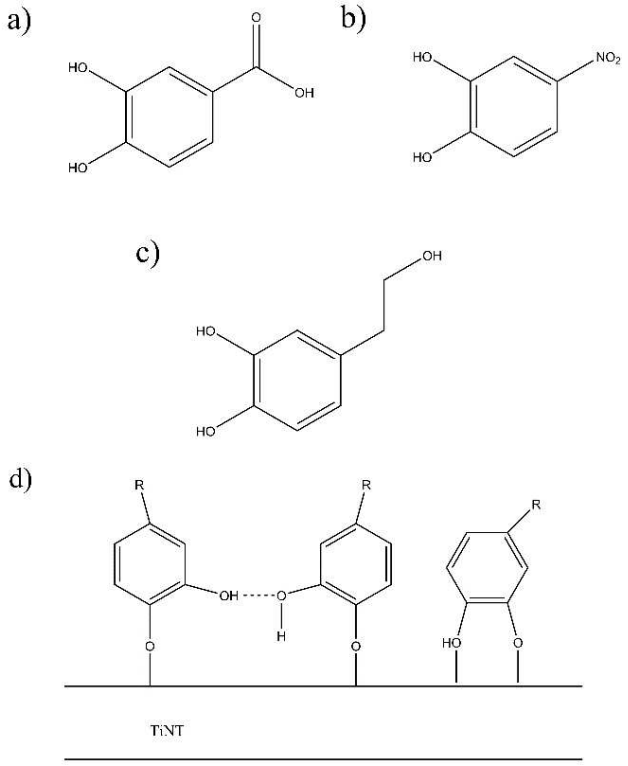

Figure 3. (a-c) structures of organic modifiers and (d) proposed general modes of attachment.

Surface Enhanced Raman Scattering

SERS is mainly observed with metallic nanoparticles, however it has been shown to occur on semiconductors.[15,16] Furthermore, Rajh and coworkers have shown SERS on TiO_2 nanoparticles attached to enediol ligands,[13,14] which occurs through the formation of a charge transfer complex. We have observed a similar enhancement on TiNT, although the enhancement is dependent on the structure of the enediol organic ligand. The formation of charge transfer complexes for all modifiers is indicated by the UV/vis spectra; the computed HOMO and LUMO positions of TiNT modified with catechol, 4-nitrocatechol and protonated dopamine are shown in Figure 4. The values of band gaps are 1.35 eV, 1.62 eV and 1.88 eV respectively. The Raman laser used in the experiments had a wavelength of 785 nm, which corresponds to 1.58 eV. Our experiments show that the TiNT-4-nitrocatechol system displays a SERS enhancement, but that the TiNT-dopamine system does not. It is reasonable that the excitation wavelength of the laser does not have enough energy to promote electrons across the band gap for the TiNT-dopamine system,(Note, however, that the computed band gap depends on the protonation state and presence of counterions, see Figure S9) resulting in no SERS effect for this system, but showing a SERS enhancement for the TiNT-4-nitrocatechol system. Without the organic modification the band gap of the TiNT system is 3.4 eV, much too large to be excited by the 785 nm laser directly.[18,26]

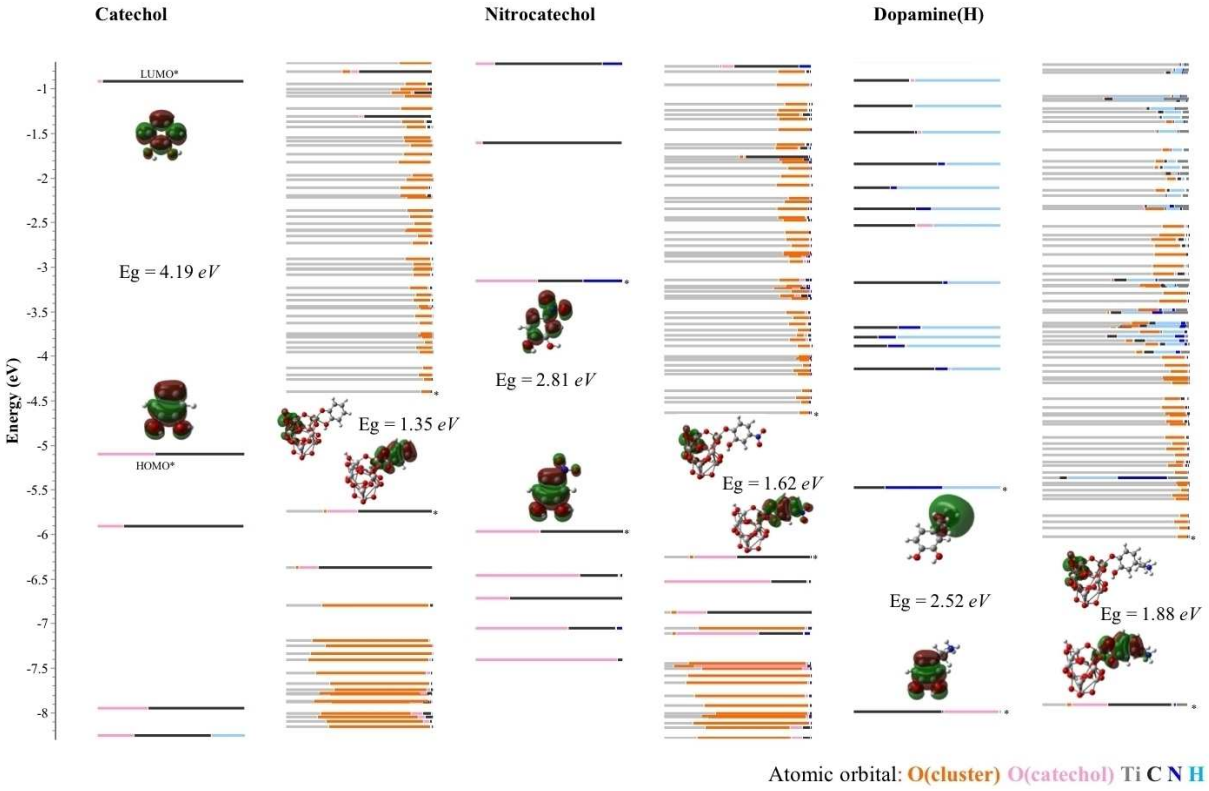

Figure 4. Molecular orbital scheme for dopants and the molecular models of dopants on TiNT (PBE level).

As can be seen in Figure 5 a and b, an enhanced Raman signal is observed for TiNT-4-nitrocatechol and TiNT-3,4-dihydroxybenzoic acid. We also expected to see an enhancement for the TiNT-dopamine and TiNT-3-hydroxytyrosol systems as they had shown similar optical profiles in the UV-vis spectra; in fact, no distinguishable peaks were observed and this is explained by the calculated band gaps.

Both the nitro and carboxylic acid substituents are electron withdrawing groups. The nitro group is a strong electron withdrawing group, whilst the carboxylic acid group is a moderate electron withdrawing group. The alkyl side chains are weak electron donating groups. This trend matches our computation results of calculated band gaps shown in Figure 4. The UV/Vis spectra does not change significantly between samples.

As a result of different substituent groups on the catechol ring, different electron densities, dipole moments and polarizability will be observed in the charge transfer complex. A greater electron withdrawing effect has shown a larger SERS enhancement in the para position in mercapto benzene derivatives.[19]

For TiNT-3,4-dihydroxybenzoic acid, five high intensity, sharp peaks are observed. Similar peaks are observed for TiNT-4-nitrocatechol, shown in Table 1. In both Raman spectra that show an enhancement, the bands can be assigned[27–29] as the phenolate C–O stretch (~1279 cm^{-1}, ν_{CO}), stretching between the two hydroxyl carbons (~1482 cm^{-1}, ν_{19b}) and skeletal modes of the benzene ring (~1330 cm^{-1}, ν_3, 1430 cm^{-1} ν_{19a} and 1584 cm^{-1}, ν_{8a} combined ν_{8b}).

Table 1. Raman peaks and assignments

TiNT- +		ν_{CO}	ν_3	ν_{19a}	ν_{19b}
3,4-dihydroxybenzoic acid	825	1279	1334	1431	1487
4-nitrocatechol	818	1278	1322	1419	1474

Bands that show enhancement for TiNT-3,4-dihydroxybenzoic acid are in the range of 1100 to 1600 cm^{-1}, which are the modes associated with ligand to metal charge transfer.[13,27,28] The peak observed in both functionalized nanotube samples at around 820 cm^{-1} is interesting. A peak is observed in 4-notrocatechol around this wavenumber, and is assigned as a NO_2 bend. There is no peak observed in 3,4-dihydrobenzoic acid or the unmodified nanotubes around this wavenumber, although the same peak is observed in both modified samples. The appearance of this band suggests that upon attachment of the modifier to the nanotube surface the symmetry of the surface is altered, allowing this band to be observed, and is therefore proposed to be Ti-O–Ti framework stretching.

Transmission electron microscope (TEM) images shown in Figure S4 are representative of the modified nanotubes, and show a thin amorphous coating of 1–2 nm. CHN analysis for the three modified materials is shown in Table S1. The surface coverages are calculated assuming a coverage of 19.6 $Å^2$ for the enediol ligands, with a BET surface area of 249.4 m^2/g. The

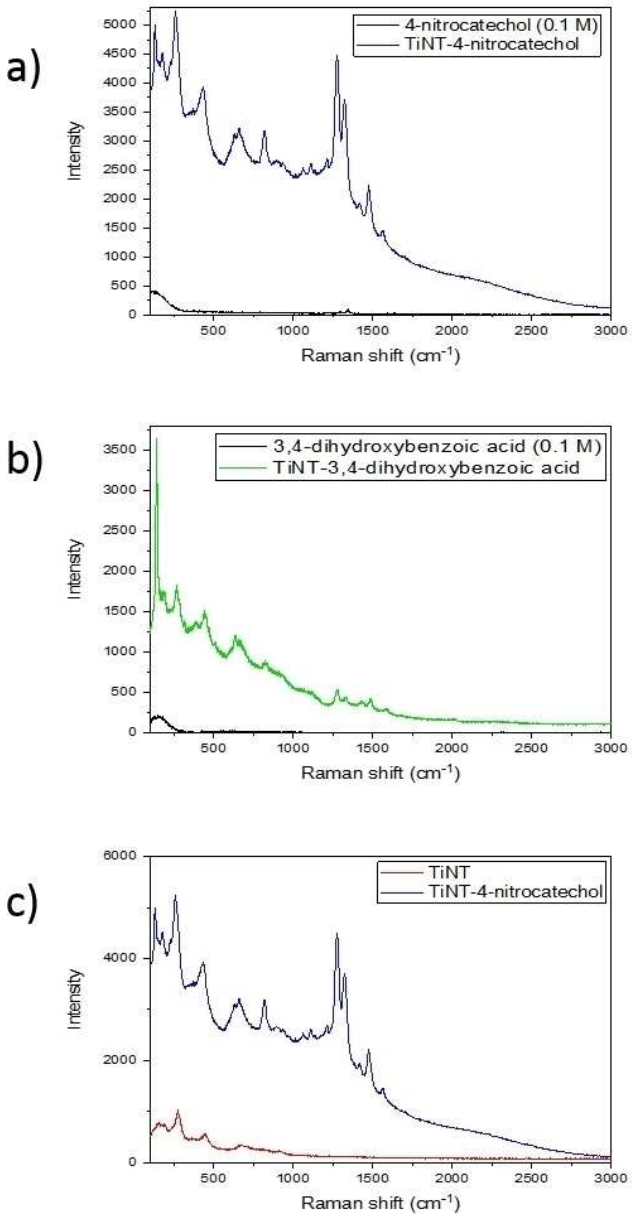

Figure 5. (a) and (b) Raman spectra for modified TiNT, modifier spectra without TiNT also shown for comparison. (c) Raman spectra of TiNT and TiNT-4-nitrocatechol.

internal surface area of the nanotube will not be available for functionalization, resulting in the observed external surface coating. All samples have a surface coverage on the same order of magnitude, ranging from 12 to 6%.

Also shown in Figure 5 a and b are the Raman signals observed for 3,4-dihydrobenzoic acid and 4-nitrocatechol at concentrations of 0.1 M. This concentration equates to a wt% of 1.5% for the two modifiers, which is of a similar magnitude to the modified TiNT samples. Compared to this concentration, the enhancement of signal is ~ 10 fold for TiNT-3,4-dihydrobenzoic acid and ~75 fold for TiNT-4-nitrochatechol. In Figure 5 c we can observe the Raman spectra for the unmodified TiNT along with the spectra forTiNT-4-nitrocatechol, which also confirms that the enhancement in signal is due to the attached organic modifier.

The enlarged Raman spectra for 0.1 M 3,4-dihydroxybenzoic acid is shown in Figure S3 for reference.

Conclusions

In this study the structure and SERS enhancement of trititanate nanotubes modified with enediol ligands was investigated, and it was found that the functional group dramatically affects the enhancement observed. When 4-nitrocatechol and 3,4-dihydroxybenzoic acid were attached to the nanotubes, a functional group attached directly to the benzene ring, a SERS enhancement is seen. In contrast, when the functional group is attached via a carbon chain, in the case of 3-hydroxytyrosol and dopamine, no signal is seen. Calculated band gaps for the TiNT-4-nitrocatchol and TiNT-dopamine systems suggest that the laser energy is the limiting factor in whether a SERS enhancement is seen. The attachment was investigated by solid state NMR and UV/Vis spectroscopy and offers further insights into catechol coatings of nanomaterials and SERS by the chemical method.

Supporting Information Summary

The supporting Information contains details of the experimental methods and computational details. Supporting computational results are presented, as well as XRD patterns and TEM images of the composites.

Acknowledgements

This work is supported by Xi'an Jiaotong Liverpool University research development fund (RDF- RDF-16-01-06), SURF projects and National Natural Science Foundation of China (Grant No. 21650110446). MB thanks EaStCHEM for support and access to a computing facility maintained by H. Früchtl. ZK gratefully acknowledges a scholarship from the Chinese Scholarship Council. SEA thanks the EPSRC for support (EP/M022501/1).

Conflict of Interest

The authors declare no conflict of interest.

Keywords: SERS · nanotubes · surface modification

[1] R. Tenne, L. Margulis, M. Genut, G. Hodes, *Nature* **1992**, *360*, 444–446.
[2] Y. Feldman, E. Wasserman, D. J. Srolovitz, R. Tenne, *Science* **1995**, *267*, 222–225.
[3] P. Hoyer, *Langmuir* **1996**, *12*, 1411–1413.
[4] A. Fujishima, K. Hashimoto, T. Watanabe, *TiO_2 Photocatalysis: Fundamentals and applications,* BKC, Tokyo, **1999**.
[5] T. Kasuga, M. Hiramatsu, A. Hoson, T. Sekino, K. Niihara, *Langmuir* **1998**, *14*, 3160–3163.
[6] A. Thorne, A. Kruth, D. Tunstall, J. T. S. Irvine, W. Zhou, *J. Phys. Chem. B.* **2005**, *109*, 5439–5444.
[7] Q. Chen, W. Zhou, G. Du, L.-M. Peng, *Adv. Mater.* **2002**, *14*, 1208–1211.
[8] S. Zhang, L.-M. Peng, Q. Chen, G. H. Du, G. Dawson, W. Zhou, *Phys. Rev. Lett.* **2003**, *91*, 256103.

[9] D. V. Bavykin, J. M. Friedrich, F. C. Walsh, *Adv. Mater.* **2006**, *18*, 2807–2824.
[10] G. Dawson, J. Liu, L. Lu, W. Chen, *ChemChatChem* **2012**, *4*, 1133–1138.
[11] R. Liu, X. Fu, C. Wang, G. Dawson, *Chem. Eur. J.* **2016**, *22*, 6071–6074.
[12] J. R. Lombardi, R. L. Birke, *Acc. Chem. Res.* **2009**, *42*, 734–742.
[13] S. J. Hurst, H. C. Fry, D. J. Gosztola, T. Rajh, *J. Phy. Chem. C* **2011**, *115*, 620–630.
[14] A. Musumeci, D. Gosztola, T. Schiller, N. M. Dimitrijevic, V. Mujica, D. Martin, T. Rajh, *J. Am. Chem. Soc.* **2009**, *131*, 6040–6041.
[15] Hayashi, R. Koh, Y. Ichiyama, K. Yamamoto, *Phys. Rev. Lett.* **1988**, *60*, 1085–1088.
[16] Y. Wang, Z. Sun, H. Hu, S. Jing, B. Zhao, W. Xu, C. Zhao, J. R. Lombardi, *J. Raman Spectrosc.* **2007**, *38*, 34–38.
[17] Z. Q. Tian, B. Ren, D. Y. Wu, *J. Phys. Chem. B* **2002**, *106*, 9463–9483.
[18] X. Wang, W. Shi, G. She, L. Mu, *Phys.Chem. Chem. Phys.* **2012**, *14*, 5891–5901.
[19] L. Yang, X. Jiang, W. Ruan, B. Zhao, W. Xu, J. R. Lombardi, *J. Phys. Chem. C* **2008**, *112*, 20095–20098.
[20] V. Biju, *Chem. Soc. Rev.* **2014**, *43*, 744–764.
[21] J. Cai, V. Raghavan, Y. J. Bai, M. H. Zhou, X. L. Liu, C. Y. Liao, P. Ma, L. Shi, P. Dockery, I. Keogh, H. M. Fan, M. Olivo, *J. Mater. Chem. B* **2015**, *3*, 7377–7385.
[22] J. Chao, W. Cao, S. Su, L. Weng, S. Song, C. Fan, L. Wang, *J. Mater. Chem. B* **2016**, *4*, 1757–1769.
[23] X. Zhu, Y. Liu, P. Li, Z. Nie, J. Li, *Analyst* **2016**, *141*, 4541–4553.
[24] K. Huo, B. Gao, J. Fu, L. Zhao, P. K. Chu, *RSC Adv.* **2014**, *4*, 17300–17324.
[25] J. Y. Huang, Y. K. Lai, F. Pan, L. Yang, H. Wang, K. Q. Zhang, H. Fuchs, L. F. Chi, *Small* **2014**, *10*, 4865–4873.
[26] P. Tarakeshwar, D. Finkelstein-Shapiro, T. Rajh, V. Mujica, *Int. J. Quant. Chem.* **2011**, *111*, 1659–1670.
[27] N. S. Lee, Y. Z. Hsieh, R. F. Paisley, M. D. Morris, *Anal. Chem.* **1988**, *60*, 442–446.
[28] S. Salama, J. D. Stong, J. B. Nielands, T. G. Spiro, *Biochemistry* **1978**, *17*, 3781–3785.
[29] J. P. Cornard, Rasmiwetti, J. C. Merlin, *Chem. Phys* **2005**, *309*, 239–249.

Submitted: June 12, 2018
Accepted: July 17, 2018

